Automotive localization integrity using proprioceptive and pseudo-ranges measurements

Olivier Le Marchand, Philippe Bonnifait, Javier Ibañez-Guzmán, David Betaille

Automotive Localization Integrity using Proprioceptive and Pseudo-Ranges Measurements

Olivier Le Marchand[1], Philippe Bonnifait[2], Javier Ibañez-Guzmán[1], David Bétaille[3]
[1]*Renault SA, Guyancourt, France*
[2]*Heudiasyc UMR 6599, Université de Technologie de Compiègne (UTC), France*
[3]*Laboratoire Central des Ponts et Chaussées (LCPC), Nantes, France*

***Abstract*—Integrity is an attribute of the quality of performance of a positioning technology that is getting crucial for many Intelligent Transportation Systems dealing with safety. Managing the confidence in estimated locations is difficult when operating in complex outdoors environments, particularly for Global Navigation Satellite Systems (GNSS). A common integrity process consists in removing outliers amongst the measurements using Fault Detection and Exclusion (FDE) algorithms and then to compute Protection Levels (PL) that quantify the integrity zone. This snapshot paradigm is applicable mainly to the aerospace domain where high pseudo-ranges redundancy exists, which is not the case for land applications. In this paper, a new approach to localization integrity for land mobile robot is proposed by combining vehicle and GNSS data, stored within a short-term memory, called data horizon. This formulation allows for the application of FDE algorithms on the combined data set. It also leads to a gain of redundancy that enables PLs to be reduced and to increase the availability of integrity algorithms. Results from evaluation tests are included to demonstrate the validity of the approach.**

***Index Terms*—Integrity, localization, multi-sensor systems, protection levels, urban environments.**

I. Introduction

When evolving outdoors, the main source of absolute position information originates at GNSS. Therefore, when occlusion or signal multipath occurs, these will result in inaccuracies. A thorough performance evaluation of GNSS receivers operating in standard traffic conditions has shown that the standard deviations recorded from the receivers do not reflect the true error of the vehicle trajectory [1]. As a result, assumptions with respect to the localization accuracy provided by GPS receivers might be misleading. It is difficult to know when errors exist, this prevents the deployment of safety-related and location dependent vehicle navigation applications [2], [3].

In the civil aviation domain, the concept of integrity has been of concern since the early 90s as aircraft navigation became more dependent on GNSS. Integrity is defined as the measure of trust which can be placed in the correctness of the information supplied by the total system. It is an integral part of the Required Navigation Performance (RNP) formulation defined by the International Civil Aviation Organization to describe the safe navigation of vessels within a defined airspace.

To ensure the safe navigation of passenger vehicles, a similar approach could be adopted, by introducing the concept of integrity. At present, this measure is missing for safety critical navigation applications. Its availability will allow for deciding whether the position estimate is reliable for its intended use, and thus for the robot to decide if the location dependent applications can be performed.

Conventional approaches to integrity measurement rely on two algorithms: Fault Detection and Exclusion (FDE) to reject outliers from the measured data and the computation of the Protection Level (PL) associated to an integrity risk. These algorithms are originally suited to aerospace applications where high redundancy of data exists and faults are rare. In contrast, when navigating in urban environments, GNSS signals are occluded and thus there is seldom redundancy. Furthermore, multiple faults exists due to errors on the pseudo-ranges originating from the multipath. Consequently, these algorithms have to be adapted for land robots localization, and GNSS combined to dead-reckoning. It shall be then possible to apply the Integrity concept to these moving platforms.

This paper proposes a new approach that combines vehicle ego-state information with GNSS data. It introduces the use of a data horizon, as a short term memory used to store measurement data, on which integrity algorithms are adapted. The formulation exploits the complementary features and redundancies of GNSS and vehicle measurements and applies the FDE algorithms to both. The use of past measurements through the data horizon and two different uncorrelated data sources decreases the protection levels. Finally, the redundancy gain allows for the application of the integrity algorithms more often than when only relying on GNSS data.

The remainder of the paper is organized as follows: Section II presents FDE and PL algorithms developed in the aerospace domain for background purposes. Section III introduces the ground vehicle specificities found in complex urban environments applied to localization systems. The principles of the proposed formulation are described in Section IV. The application of the new formulation to passenger vehicles using GNSS based localization system is presented in Section V. The validation of the proposed approach is included in Section VI. A critique of the results and its applicability to navigation tasks are given in Section VII.

II. Fault Detection and Exclusion & Protection Level Algorithms

The principles of localization integrity were first introduced in a standardized manner as part of the Global Positioning System (GPS). In ideal conditions, disturbances, such as multipath, are assumed to be non existent, so the system is considered "fault free", leading to results considered as having high integrity. In this context, a fault is defined as "an unacceptable deviation of at least one characteristic property of the system from standard conditions". For ground vehicles, multipath are considered as GNSS faults, as well as a wheel slippage when using wheel speed sensors. To remove these faults, FDE algorithms based on measurement redundancy are applied. Next, the degree of trust that can be placed in the location estimates is calculated. This is represented by protection levels (PL) [4]. This section briefly presents the computation of FDE for GNSS, i.e. Receiver Autonomous Integrity Monitoring (RAIM) algorithm, and PL algorithm for background purposes.

A. RAIM Algorithm

This algorithm is applicable to any redundant measurement system. It has to be noticed that the presence of only one fault at a time is assumed. First it uses a least square resolution applied to a linearized observation equation:

$$Y = h(X) \Rightarrow dY = H.dX \tag{1}$$

where Y is the exteroceptive measurement vector (in GPS, pseudo-range vector for instance), X is the pose vector, dY and dX the respective linearized vectors. The noise on Y is supposed to be independent, Gaussian and zero mean with known variance Q_Y. H is the Jacobian of the observation function h at the linearization point X_0. The estimated linearized state dX is given by:

$$d\hat{X} = \left(H^T Q_Y^{-1} H\right)^{-1} H Q_Y^{-1} \cdot dY \hat{=} H^+ \cdot dY \tag{2}$$

where H^+ is the weighted pseudo-inverse of matrix H. The residuals ε can be calculated as the difference between the measurements and the "estimated measurements" $h(\hat{X})$; these are derived from the estimated state:

$$\varepsilon = Y - h(\hat{X}) \approx dY - Hd\hat{X} = (I - HH^+)dY \hat{=} S \cdot dY \tag{3}$$

In normal conditions, the variable dY belongs to the Kernel of matrix S, then the mean of each component of the residual vector is centered on 0.

Now, if faults are added to the pseudo-range vector, Eq. 4 and Eq. 3 have to be rewritten:

$$d\hat{X} = H^+ \cdot (dY + E) \tag{4}$$

$$\varepsilon = S \cdot (dY + E) \tag{5}$$

where E is the vector of faults. If only one fault of magnitude b_i occurs on the *i*th pseudo-range, i.e. only the *i*th element of E is non-zero and $E(i) = b_i$, then all the components of ε are no more centered on 0. In practice, the detection is made by calculating the Sum the Squared Error (SSE), which is compared to a threshold Th equal to a χ^2distribution at $n - m$ degrees of freedom, having defined a probability of false alarm P_{fa}, where n is the number of measurements used and m the state size, $Th = \chi^2_{(1-P_{fa},n-m)}$. This outlines the need of having many measurements ($n >> m$) as it increases the degrees of freedom of the problem and makes it easier to perform detection. So, an integrity failure is detected if:

$$SSE = \varepsilon^T Q_Y^{-1} \varepsilon > Th \tag{6}$$

Once the occurrence of a fault is detected, it is necessary to identify the faulty measurement. Hence the score w_j is computed for each measurement as a function of its residual and its variance:

$$Q_\varepsilon = Q_Y - H\left(H^T Q_Y^{-1} H\right)^{-1} H^T \tag{7}$$

$$w_j = \left| \varepsilon_j / \sqrt{(Q_\varepsilon)_{j,j}} \right| \tag{8}$$

The maximum score indicates the faulty measure. This is then removed from the measurements vector, next a new position is calculated and a new detection test is performed and so on. One can notice that w_j is a normalized score that takes into account both the geometrical configuration and the measurement noise thanks to Q_ε calculation. It has to be noticed that FDE applied to GNSS needs at least 5 satellites to perform detection, and 6 satellites to perform exclusion because the state size is equal to 4.

RAIM algorithm underwent some improvement with adaptive threshold [5]. It can be based on parity space methods which present similar results due to the linear formulation [6] Nevertheless one necessary condition to apply these algorithms is the capability to represent the problem in a linear and observable manner as in Eq. 2. The performance comparison of these different methods for vehicle integrity is out of the scope of this paper.

B. Protection Level Calculation

The next step is to perform a protection level computation as it represents a possible metric for the integrity of localization. The concept of protection level answers to the following question: "What are the consequences of one undetected fault on the positioning error". If a fault occurred only on the *i*th measurement, with a magnitude equal to b_i, and computations are performed in a tangent local frame, then the error in the horizontal plane will be equal to [4] [7]:

$$e_{hor}^{i\,2} = \left(H_{(1,i)}^{+\,2} + H_{(2,i)}^{+\,2}\right) b_i^2 \tag{9}$$

In order to link this quantity to the norm of the residuals, the quantity $HSlope$ is defined. It depends on the geometrical configuration of the receiver with respect to the satellites. $HSlope_{MAX}$ represents the maximum $HSlope_i$ over all the measurements:

$$e_{hor}^i = \sqrt{\frac{\left(H_{(1,i)}^{+\,2} + H_{(2,i)}^{+\,2}\right)}{\sum_j S_{(j,i)}^2}} . \|\varepsilon_i\| \hat{=} HSlope_i . \|\varepsilon_i\| \tag{10}$$

Under the assumptions of only one fault at a time and of having a Gaussian noise of known variance on all measurements, the maximum position bias due to an undetected fault is defined as the Approximate Radius of Protection (ARP):

$$ARP = HSlope_{MAX}.Th \tag{11}$$

Finally, the effect of noise R is taken into account through the ellipsoid of the positioning error characterized by a probability of missed detection P_{md}, what leads to compute the Horizontal Protection Level (HPL):

$$HPL = HSlope_{MAX}.Th + R(P_{md}) \tag{12}$$

It has to be noticed that PL computation relies on the capability to express the observation problem with an invertible matrix, like RAIM does.

III. Ground Vehicle Localization Specificities

For ground localization, GPS is a key sensor as it is available all over the world. However, due to multipath occurrence in constrained environments, GPS positioning and RAIM performance are prone to severe deterioration. Unlike open sky aerospace conditions, passenger vehicles encounter urban areas where streets are lined of buildings. Thus it is difficult to obtain more than 7 satellites and it is often less [8].

However, vehicle localization can take benefit from vehicle specific sensors i.e. wheel speed and inertial sensors and from a priori information like digital maps of the road network [9]. It has been demonstrated that the combination of exteroceptive and proprioceptive sensors can significantly improve FDE. For instance, FDE based on an Extended Kalman filter (EKF) can perform the detection and exclusion of outliers in GPS measurements [10] [11] using innovation signals (sometimes called pre-residuals). However, in spite of their promising results, such techniques have been little linked to PL calculation [8]. In other words, the gain in outliers detectability has not been turned into a gain in the integrity metric. Actually, the estimation state from the update equation of the EKF is a function of the current measurements and the last estimated state, Eq. 13. Thus, it can be impacted by a biased predicted state due to faults occuring on the past measurements. But such a consequence cannot be straightforward evaluated, like in Eq.9, because all the past measurements are mixed up in $X_{k|k-1}$. Therefore protection levels can not be computed.

$$X_{k|k} = X_{k|k-1} + K_k\left(Y_k - HX_{k|k-1}\right) \tag{13}$$

For these reasons, we propose in the following to consider data horizon in order to process a short term history of the trajectory, sometimes called finite memory approach.

IV. Trajectory Monitoring Algorithm

A. Data Horizon Principle

Data horizon is one possible estimation method to combine proprioceptive and exteroceptive data and it has already been used in diagnosis [12][13]. The principle is to stack consecutive states, then to estimate them together. The usual method consists in

- Using a discrete linearized model:

$$\begin{cases} X_k = AX_{k-1} + BP_k \\ Y_k = HX_k \end{cases} \tag{14}$$

- Stacking over time the states in one side, the measurement vector Y_k and input vector P_k in the other side. For instance, if matrix B can be pseudo-inverted, stacking two states leads to Eq. 15:

$$\begin{bmatrix} Y_k \\ P_k \\ Y_{k-1} \end{bmatrix} = \begin{bmatrix} H_k & 0 \\ B_k^+ & -B_k^+ A_k \\ 0 & H_{k-1} \end{bmatrix} . \begin{bmatrix} X_k \\ X_{k-1} \end{bmatrix} \tag{15}$$

If the so composed matrix is full rank, then it can be pseudo-inverted, and it is clearly compatible with the formulation expressed in Eq. 2. Hence RAIM algorithm can be applied and PL computed. However this data horizon formulation presents a main drawback: it is not possible to separate input sensor failures from evolution model failures, because matrix A which contains the evolution constraints is involved in the expression of P_k. Hence another formulation has to be thought separating evolution model and input sensor model.

B. Trajectory Observation Formulation

Since we only address an observation problem, there is no need to use a state space formulation similar to Eq. 14. In fact, proprioceptive measurements (usually placed in the input vector P_k) can be considered as observations of the traveled trajectory and the evolution model as constraints on it. As they measure or provide a priori information on the movement of the robot or its derivatives, they can be expressed as functions of the state derivatives in the continuous case or as functions of two or several consecutive states in the discrete case:

$$\begin{cases} \vec{0} = l\left(X_{k-q}, ..., X_k\right) \\ P_k = g\left(X_{k-r}, ..., X_k\right) \\ Y_k = h\left(X_k\right) \end{cases} \tag{16}$$

where g and l are respectively the new expressions of the proprioceptive sensor model and of the evolution model with respect to the trajectory. In contrast to the previous Data Horizon method, this new formulation leads to express the whole trajectory observation problem in a non linear manner, then to linearize around a given trajectory, which gives:

$$\begin{bmatrix} \vec{0} \\ d\tilde{P} \\ d\tilde{Y} \end{bmatrix} = \begin{bmatrix} \frac{\partial l}{\partial \tilde{X}}\Big|_{\tilde{X}_0} \\ \frac{\partial g}{\partial \tilde{X}}\Big|_{\tilde{X}_0} \\ \frac{\partial h}{\partial \tilde{X}}\Big|_{\tilde{X}_0} \end{bmatrix} .d\tilde{X} \tag{17}$$

where $d\tilde{P}$, $d\tilde{Y}$, $d\tilde{X}$ are respectively linearized horizon of adapted depth of proprioceptive measures, exteroceptive measures and position. To compare with the previous formulation, stacking two states leads to:

$$\begin{bmatrix} Y_k \\ 0 \\ P_k \\ Y_{k-1} \end{bmatrix} = \begin{bmatrix} H_k & 0 \\ \partial l/\partial X_k & \partial l/\partial X_{k-1} \\ \partial g/\partial X_k & \partial g/\partial X_{k-1} \\ 0 & H_{k-1} \end{bmatrix} \cdot \begin{bmatrix} X_k \\ X_{k-1} \end{bmatrix} \tag{18}$$

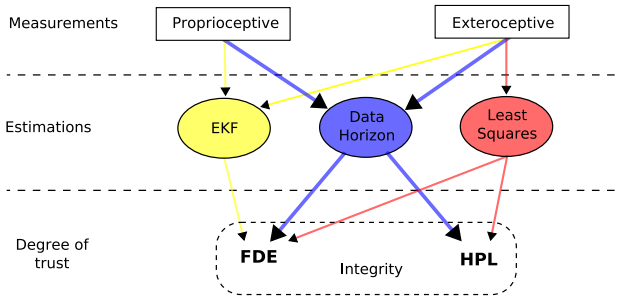

Figure 1. Applicability of integrity to sensor types regarding data fusion schemes

Like for the previous formulation, RAIM algorithms can be applied and protection levels computed. The major difference is that FDE can be independently performed on the proprioceptive measurements P_k and the evolution model (this being represented through constraints equal to 0). The protection level includes the whole trajectory stored in the data horizon, from which it is straightforward to extract the protection level of the current position (the last introduced in the buffer).

As represented in Figure 1, data horizon merges advantages of EKF and Least Squares together. Whilst EKF allows to apply FDE to exteroceptive sensors with the help of proprioceptive sensors and Least Squares allows to apply FDE and HPL on exteroceptive measurements, data horizon makes it possible FDE and HPL computation on both exteroceptive and proprioceptive measurements. So it perfectly matches an automotive integrity scheme.

As it extends integrity to proprioceptive sensors, the global redundancy is increased compared to FDE algorithms applied separately at each time step with Least Squares. This can be justified by comparing the degrees of freedom of this formulation to the sum of the degrees of freedom of individual GPS FDE. As an example, if there are 6 satellites in view and a 4-size state, there are 2 degrees of freedom for a usual χ^2test of a RAIM algorithm. If a 4-samples data horizon is used with 2 proprioceptive sensors and one evolution constraint there are a maximum of 33 measurements for a 16-size state, so there are 17 degrees of freedom compared to 4 times 2 degrees of freedom with individual FDE. This increase of redundancy allows to enhance the performance of FDE algorithms and to apply them even when there are few exteroceptive measurements, for example when less than 5 satellites are visible, preventing usual RAIM computation.

The impact of a fault on the horizontal positioning error, e_i, depends on its magnitude and on the weight of the measurement in the position estimation. With respect to a one epoch Least Squares, data horizon decreases the weight of each exteroceptive measurement at this epoch because they are linked to the exteroceptive measurements at previous epochs through the proprioceptive data and the evolution model. Consequently $HSlope_{MAX}$ is lower. This does not seem to be compensated by the Th increase (due to the degree of freedom rise), so ARP is reduced, as exposed in Section VI.

The following section will present a test case.

V. Application to Passenger Car Localization

The formalized strategy based on Eq. 17 has been applied to the localization of a car vehicle equipped with two wheel speed sensors, a yaw rate gyro, a GPS receiver, and under the assumption of a constant altitude evolution model. For simplification this section presents only part of the developed model. The GPS model is the same as usually used in tight coupling, so formulas and their linearization are not expressed and can be found in [11]. The state is expressed here in a earth-tangential local frame with a Cartesian coordinates system. The location is augmented by the clock bias of the receiver for each epoch, thus:

$$X_k^a = \begin{bmatrix} x_k & y_k & z_k & cdt_k \end{bmatrix}^T \tag{19}$$

Considering the position of the car as the center of the rear axle, the speed of a wheel (here the rear left at time k: $v_{rl,k}$) is a function of the distance traveled by the rear axle center corrected by the difference of speed between left and right wheel due to the turning maneuver:

$$v_{rl,k}=g_{rl}\left(X_k^a,X_{k-1}^a,X_{k-2}^a\right)=\frac{\left(d_k-\frac{L(\theta_k-\theta_{k-1})}{2}\right)}{\Delta t_k} \tag{20}$$

where d_k is the distance traveled between two epochs, θ_k the current heading, L the width of the rear axle and $\Delta t_k = t_k - t_{k-1}$. Assuming a 2D motion in the horizontal plane and a sufficient sampling of the trajectory, d_k and θ_k, can be expressed as:

$$d_k = \sqrt{\left(x_k - x_{k-1}\right)^2 + \left(y_k - y_{k-1}\right)^2} \tag{21}$$

$$\theta_k = atan2\left(\left(y_k - y_{k-1}\right), \left(x_k - x_{k-1}\right)\right) \tag{22}$$

Then it can be easily derived:

$$\frac{\partial d_k}{\partial X_k^a} = G_k^d = \begin{bmatrix} \frac{(x_k - x_{k-1})}{d_k} & \frac{(y_k - y_{k-1})}{d_k} & 0 & 0 \end{bmatrix} \tag{23}$$

$$\frac{\partial \theta_k}{\partial X_k^a} = G_k^\theta = \begin{bmatrix} \frac{-(y_k - y_{k-1})}{d_k^2} & \frac{(x_k - x_{k-1})}{d_k^2} & 0 & 0 \end{bmatrix} \tag{24}$$

$$\frac{\partial g_{rl}}{\partial X_k^a} = G_{k,0}^{rl} = \frac{G_k^d + L.G_k^\theta L.G_k^\theta/2}{\Delta t_k} \tag{25}$$

$$\frac{\partial g_{rl}}{\partial X_{k-1}^a} = G_{k,1}^{rl} = \frac{-2G_k^d - L.G_{k-1}^\theta - L.G_k^\theta}{2\Delta t_k} \tag{26}$$

$$\frac{\partial g_{rl}}{\partial X_{k-2}^a} = G_{k,2}^{rl} = \frac{L.G_{k-1}^\theta}{2\Delta t_k} \tag{27}$$

The introduction of an evolution model can be done in the same way. For example, if the altitude has to be constrained as a constant (in order to improve bad stability of GPS altitude) a simple equation can be added:

$$0 = l_{dz}\left(X_k^a, X_{k-1}^a\right) = z_k - z_{k-1} \tag{28}$$

Figure 2. Test trajectory at Compiègne - France

Here is an example of the full trajectory observation matrix with a 4-samples state horizon, a GPS sensor, a rear left wheel speed sensor, and a constant altitude constraint:

$$\begin{bmatrix} 0 \\ 0 \\ 0 \\ dv_{rl,k} \\ dv_{rl,k-1} \\ d\rho_k \\ d\rho_{k-1} \\ d\rho_{k-2} \\ d\rho_{k-3} \end{bmatrix} = \begin{bmatrix} L^{dz} & -L^{dz} & 0 & 0 \\ 0 & L^{dz} & -L^{dz} & 0 \\ 0 & 0 & L^{dz} & -L^{dz} \\ G^{rl}_{k,0} & G^{rl}_{k,1} & G^{rl}_{k,2} & 0 \\ 0 & G^{rl}_{k-1,0} & G^{rl}_{k-1,1} & G^{rl}_{k-1,2} \\ H_k & 0 & 0 & 0 \\ 0 & H_{k-1} & 0 & 0 \\ 0 & 0 & H_{k-2} & 0 \\ 0 & 0 & 0 & H_{k-3} \end{bmatrix} \begin{bmatrix} dX^a_k \\ dX^a_{k-1} \\ dX^a_{k-2} \\ dX^a_{k-3} \end{bmatrix} \quad (29)$$

where ρ is the pseudo-range vector and:

$$L^{dz} = \begin{bmatrix} 0 & 0 & 1 & 0 \end{bmatrix} \quad (30)$$

This simple example provides a mathematical formalization of our data horizon approach.

VI. Results

The results of the experiments performed to validate the proposed approach are presented in this Section. For this purpose the trajectory of a passenger vehicle, whose satellite view is depicted in Figure 2, and ego-state variables were recorded together with data from an automotive-type GPS, in real traffic conditions. The ego-states variables are extracted from the rear wheel speeds and a yaw rate gyroscope. The vehicle was driven for a distance of 2.5 km in an urban context. This data was processed off-line and faults introduced on the pseudo-ranges to emulate their occurrence, as described in [11]. The introduction of the faults allows to run the algorithms with the certainty of their existence, as their detection is one of the objectives. FDE and PL algorithms are then applied to this data set.

Results are shown in Figure 3, the vehicle travels in a straight line at 20 m/s. Only the 6 higher satellites are considered into the GPS measurements. The length of the data horizon chosen was 8 samples according to the vehicle dynamic. To simulate the occurrence of faults, a bias of 15m was introduced to the pseudo-range of the same satellite, for the last two samples. A false alarm probability of 0.001 was taken. The measurements on the true trajectory are represented by diamonds (green color). The circles (blue color) represent the positions estimated applying the data horizon based algorithms. The crosses (color red) are the positions estimated independently at each sample with the conventional RAIM algorithm applied to GPS data. The figure presents a typical behavior of an iterated RAIM algorithm applied to the proposed formulation when multiple faults exist. It can be remarked that the last two crosses have a larger error due to the fault introduced onto one of the pseudo-ranges. The FDE algorithm on the GPS only estimation can not detect the error due to the low bias magnitude.

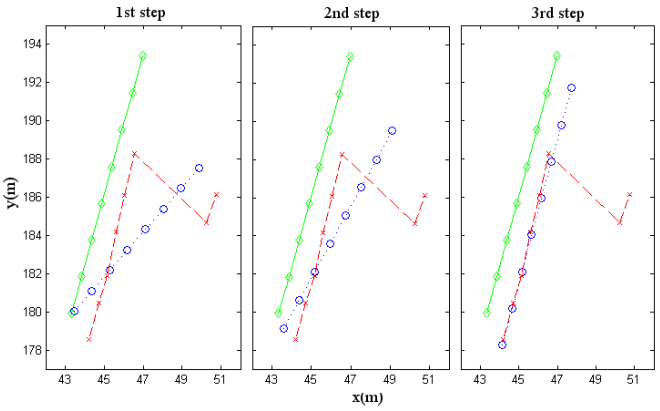

Figure 3. Consecutive steps of data horizon based FDE

Figure 3, shows three steps that represent the consecutive use of the FDE as a results of the data horizon. The first step represents the estimation through the data horizon for all the measurements including the two biases. In the second step, an iterative RAIM algorithm is applied. This has led to the detection and removal of one of the two faults and a new trajectory estimate has been generated. For the third step a new detection and exclusion stage is performed. This results in a further correction of the trajectory estimate as shown in Figure 3. It is important to observe that the shape of the estimated trajectory using the new algorithm is continuous (no jumps). The heading is corrected gradually, the alignment between points show the contribution of the proprioceptive sensors on the estimation.

The approximate radius of protection was computed for the whole trajectory, taking into account 7 satellites for a data horizon depth of 8 samples. The results are shown in Figure 4. The variations in the ARP during the trajectory are due to the vehicle speed and yaw rotation. It is observed that a long straight line at 70km/h leads to the lowest ARP between $t = 200s$ and $t = 500s$. This configuration is well-suited for reducing position uncertainty by benefiting of the position filtering. It allows for the reduction in the ARP. By contrast moving at low speeds with the vehicle in a turning maneuver (e.g. crossing a round about) leads to a high ARP, as what occurs between $t = 0s$ and $t = 250s$.

The absolute value of the ARP is due to other factors than the vehicle response. First, the more satellites are in view, the lower will be the ARP. Second, the deeper the data horizon, the lower the ARP. Figure 5 shows this observation. It presents the ARPs computed for different horizon depths. The contributions of the measurements by the proprioceptive sensors and evolution models described in Section IV can be

observed. Further, the gain is non-linear with regard to the data horizon depth, and it seems to reach a limit: adding old measurements provides less and less information. The probability of false alarm (10^{-3}) used to set the detection threshold has an impact on the absolute value. This might not be sufficient to address safety applications, however, a a higher value leads to meaningless protection levels in the case of passenger vehicle applications. It is envisaged that the ARPs obtained could be HPL compatible with applications like road-tolling where the liabilities are economical rather than safety related.

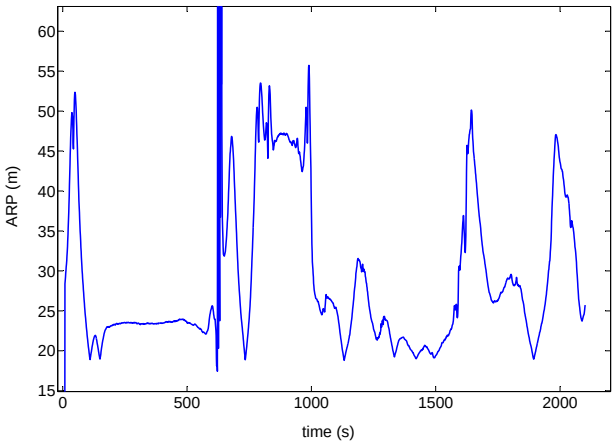

Figure 4. ARP of the current location on the whole test trajectory

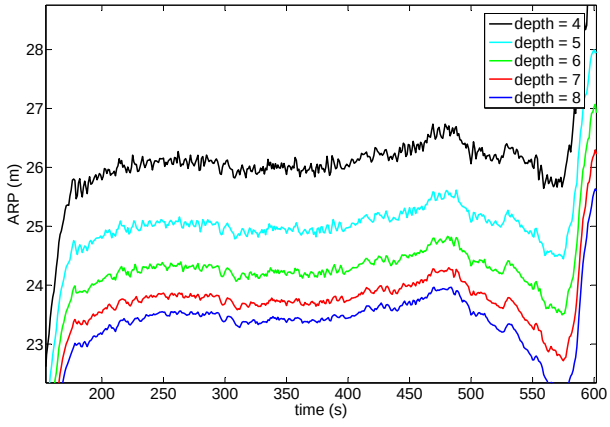

Figure 5. ARP comparison for different horizon depths

VII. Conclusion

Conventionally, integrity measures of localisation systems have been limited to the aerospace domain and centered on GPS measurements. In this paper, through a new formulation that incorporates vehicle ego-state data, it was possible to extend them to mobile ground Intelligent Transportation Systems applications. The proposed approach uses past information and provides an adapted formulation for FDE and PL algorithms. FDE algorithms are therefore applied not only to GPS measurements but include vehicle ego-state measurements and the evolution model. Another advantage is the reduction of the PL with the help of these new data. This formulation increases data redundancy availability and therefore extends the usage of FDE and PL algorithms throughout most of the vehicle trajectory.

The experimental results have shown that it is possible to compute the ARP and to detect faults for outdoors mobile platforms using the proposed formulation. The algorithms perform well when moving at most speeds, except when the vehicles were at very low speed. This is due to the proximity of the positions considered as part of the data horizon which leads to singularities affecting the computation. The problem is being addressed by applying a spatial sampling rather than a temporal one.

By augmenting the evolution model through the inclusion of vehicle dynamics and adding constraints like the geometry of the traversed roads available from accurate digital road maps, it will be possible to enhance the integrity estimations. Information, which will lead to the use of localisation based solutions for safety-critical applications like guiding automatically intelligent passenger vehicles.

References

[1] J. Ibañez-Guzmán, O. Le Marchand, and C. Chen, "Metric evaluation of automotive-type GPS receivers," in *Proc. FISITA*, Munich, Germany, Sept. 2008.

[2] S. Feng and W. Ochieng, "Integrity of navigation system for road transport," in *Proc. 14th World Congress of Intelligent Transportation Systems*, Beijing, Oct. 2007.

[3] H. Durrant-Whyte, D. Pagac, B. Rogers, M. Stevens, and G. Nelmes, "An autonomous straddle carrier for movement of shipping containers," *IEEE J. Robot. Automat.*, vol. 14, pp. 14–23, Sept. 2007.

[4] T. Walter and P. Enge, "Weighted RAIM for precision approach," in *Proc. 8th International Technical Meeting of the Satellite Division of the Institute of Navigation*, Palm Springs, CA, Sept. 1995.

[5] M. A. Sturza and A. K. Brown, "Comparison of fixed and variable threshold RAIM algorithms," in *Proc. of the 3rd International Technical Meeting of the Satellite Division of the Institute of Navigation ION GPS 1990*, Colorado Spring, CO, Sept. 1990, pp. 437–443.

[6] R. G. Brown, "A baseline RAIM scheme and a note on the equivalence of three RAIM methods," in *Proc. of the 1992 National Technical Meeting of the Institute of Navigation*, San Diego, CA, Jan. 1992, pp. 127–137.

[7] B. Belabbas and F. Gass, "RAIM algorithms analysis for a combined GPS/galileo constellation," in *Proc. ION GNSS*, Palm Springs, CA, Sept. 2005.

[8] S. Hewitson and J. Wang, "GNSS receiver autonomous integrity monitoring (RAIM) performances analysis," *GPS Solutions*, vol. 10, no. 3, pp. 155–170, July 2006.

[9] C. Fouque and P. Bonnifait, "Tightly coupled GIS data in GNSS fix computation with integrity test," *International Journal of Intelligent Information and Database Systems*, vol. 2, no. 2, pp. 167–186, 2008.

[10] S. Sukkarieh, E. M. Nebot, and H. Durrant-Whyte, "A high integrity IMU/GPS navigation loop for autonomous land vehicle applications," *IEEE Trans. Robot. Automat.*, vol. 15, no. 3, pp. 572–578, 1993.

[11] O. Le Marchand, P. Bonnifait, J. Ibañez-Guzmán, F. Peyret, and D. Bétaille, "Performance evaluation of fault detection algorithms as applied to automotive localization," in *Proc. of the European Navigation Conference GNSS*, Toulouse, France, Apr. 2008.

[12] O. Adrot, D. Maquin, and J. Ragot, "Fault detection with model parameter structured uncertainties," in *European Control Conference, (ECC97)*, Karlsruhe, Germany, Aug./Sept. 1999.

[13] F. Gustafsson, "Stochastic observability and fault diagnosis of additive changes in state space models," in *Proc. IEEE International Conference on Acoustics, Speech, and Signal Processing*, Karlsruhe, Germany, 2001, pp. 2833–2836.